Moroccan Journal of Chemistry
ISSN: 2351-812X
http://revues.imist.ma/?journal=morjchem&page=login
Kali & al. / Mor. J. Chem. 10 N°3 (2022) 509-522
DOI: https://doi.org/10.48317/IMIST.PRSM/morjchem-v10i3.33140

Study of the adsorption properties of an almond shell in the elimination of methylene blue in an aquatic

A. Kali [(a)], Y. Dehmani [(a)], I. Loulidi [(a)], A. Amar [(a], M. Jabri [(a)], A. El-kord [(b)*], F. Boukhlifi [(a)]

(a) Laboratory of applied physical chemistry ability of sciences, 4010, Beni M'Hamed, Meknes, Morocco
(b) Laboratory of Materials, Membranes and Nanotechnology, PB 11201, Zitoune, Meknes, Morocco.

** Corresponding author:*
abderrazekelkordy@gmail.com
Received 14 April 2022
Revised 14 Jun 2022
Accepted 20 Jun 2022

Abstract

The discharges of many industries are loaded with dyes that pose a major problem for health and the environment. Various techniques and methods (physical, chemical, biological...) were developed for the treatment of the effluents charged in dyes. Adsorption is one of the most suitable techniques for the removal of dyes, and natural wastes are among the most used materials as adsorbents. This work is based on the study of the removal of methylene blue in an aqueous medium, using almond shells as adsorbents. The support used was characterized by X-ray diffraction, Scanning electron microscopy, BET method, and Infrared spectroscopy. The results obtained showed that the adsorption equilibrium is established after 20 minutes. We also evaluated the effect of parameters such as pH effect, mass effect, temperature effect, and particle size effect. The equilibrium adsorption kinetics shows that this support has good retention for methylene blue. The adsorption isotherm obtained is described by the Freundlich model and this adsorption follows a pseudo-second-order equation. The thermodynamic parameters show that the process is endothermic, spontaneous, and disordered.

Keywords: *adsorption, almond shells, methylene blue, isotherm, adsorption parameter*

1. Introduction

Dyes are used in many industrial sectors, such as the textile, paper, leather, food, and cosmetics industries [1]. Dyes are known to be toxic and persistent in the environment [2]; Physical and chemical techniques are needed to degrade them. Methylene blue is the most commonly used dye in cotton dyeing wood and silk. It can cause eye burns and cause injury it is eternal to human and animal eyes. Inhalation can cause Difficulty breathing and burning sensation if ingested through the mouth, causing nausea, vomiting, sweating, and a lot of cold sweat [3]. There has been a great deal of interest in the treatment of industrial waste containing this dye. A variety of physical, chemical, and biological technologies has been developed and tested Used to treat wastewater containing dye. These procedures include flocculation, precipitation, ion exchange, membrane filtration, irradiation, and zonation. However, these procedures are expensive and lead to a large number of sludge formations or drift [4]. In the process of treating liquid discharges, adsorption is still a more commonly used and easy-to-use technology. Activated carbon is the most absorbent Due to its high adsorption capacity for organic matter; it is widely used [5]. However, such adsorbents are expensive and difficult to regenerate. In search of another, therefore, an effective and less expensive adsorbent is of interest. In Morocco, thanks to the Green Morocco Program, we have witnessed the obvious development of the almond industry, the national production of almonds reaches 101 thousand tons each year. The almonds are harvested by hand. The by-product "almond shell" represents 75 to 80% of the biomass and constitutes an exploitable agricultural resource, unfortunately of low value. This research work is an initiative to develop almond shell raw material aggregates as adsorbents for chemical dyes, which pollute wastewater from the textile and agricultural industry [6], [7].

2. Materials and methods

2.1 Adsorbent Almond shells

The almond is the fruit of the almond tree (family Rosaceae) consisting of a whitish oval seed, covered with a brown layer, which is in a fibrous shell bursting at maturity. The biomass samples studied are collected from different regions of Morocco. The shells obtained are washed several times with distilled water in order to eliminate any kind of dust or adhering impurities until clear washing water is obtained, and dried for 24 hours at a temperature of 110 °C in an oven. Then the shells were crushed and sieved to obtain finer and more homogeneous samples (to increase its specific surface).

2.2 Methods

100 mg of almond shell is taken and brought into contact with a volume of 20 mL of the aqueous solution of MB dye (15 mg /l). The mixture is stirred for contact times ranging from 20 to 300 min at 400 rpm. The solutions are then filtered on a 0.45µm microporous membrane and the filtrates obtained are analyzed by UV/Visible spectrophotometry at a wavelength of 670 nm. The amount of the MB dye adsorbed in ($mg.g^{-1}$) was calculated using the equation [8]:

$$q_e = \frac{Co - Ct}{m} V \quad (1)$$

C0 and Ce are the initial and the equilibrium concentrations of MB dye in mg/L; m is the mass of adsorbent in g; V is the volume of MB dye solution in mL; and qe ($mg.g^{-1}$) is the equilibrium concentration of MB dye.

The adsorption isotherms were conducted at room temperature, by dispersing suspensions of 100 mg of solid in 20 mL of MB solution at initial concentrations ranging from 15mg/l up to 60mg/l without pH adjustment. After equilibration time, the suspensions were centrifuged and the supernatants were measured by the method mentioned above eq **(1)**.

The influence of pH was studied in the range of 2 to 13 on almond shell solid suspensions. 20 mL of a MB dye solution (40mg/l) is brought into contact with 100 mg of adsorbent. Then, the suspensions are stirred for 3 hours while

adjusting the pH to the required value by adding hydrochloric acid or soda (0.01N). During the experiments, we have respected equilibrium times for the interaction of the dye with the adsorbent. The dye concentrations and adsorbent mass are very significant factors for effective adsorption. To illustrate the effect of dye concentration on the adsorption, experiments were performed at different dye concentrations. A mass of 100 mg of adsorbent was brought into contact with 20 mL of the dye solution in different time intervals.

Kinetic and isothermal modelling

In order to determine the mechanism of adsorption of methylene blue on almond shell, we use the mathematical forms of the kinetic and isotherm models well known in the literature [5-7]. Indeed, the adsorption kinetics is modeled using the pseudo-first order, pseudo-second order and intra-particle Weber-Morris models:

Pseudo-first order kinetics model [8]:

The non-linear form:

$$\frac{dq_t}{dt} = k_1 * (q_e - q_t) \quad \textbf{(2)}$$

The linear form:

$$\ln(q_e - q_t) = \ln q_e - k_1 * t \quad \textbf{(3)}$$

Where: qe is the adsorption capacity- at equilibrium (mg.g^{-1}), qt is the adsorption capacity at time t (mg.g^{-1}), t is the contact time (min), k_1 is the adsorption rate constant for the pseudo-first order (min^{-1}).

Pseudo-second order kinetics model [9]:

The non-linear form:

$$\frac{dq_t}{dt} = k_2 * (q_e - q_t)^2 \quad \textbf{(4)}$$

The linear form:

$$\frac{t}{q_t} = \frac{1}{k_2 * q_e^{\,2}} + \frac{t}{q_e} \quad \textbf{(5)}$$

Where: k_2 is the adsorption rate constant for pseudo-second order (g.mg^{-1}.min^{-1}) and qe is the adsorption capacity at equilibrium (mg.g^{-1}),

The intra-particle diffusion model:

The intra-particle diffusion model is proposed by Weber and Morris [10]. The limiting step in the adsorption process is determined using this model. The expression of this model is expressed by equation:

$$q_t = k_d * t^{0.5} + C \quad \textbf{(6)}$$

Where kd is the intraparticle diffusion constant in (mg.g^{-1}.min$^{-1/2}$) and C is a constant that characterizes diffusion of the solute into the liquid phase.

While those of the isotherms were confronted by the Langmuir and Freundlich models:

Langmuir model: The Langmuir model [28], is given by the following equation:

$$q_e = \frac{q_{max} * (k_L * C_e)}{(1 + k_L * C_e)} \quad \textbf{(7)}$$

Where: qe is the equilibrium adsorbed quantity (mg/g), Ce is the equilibrium concentration (mg/L), K_L is Langmuir's equilibrium constant (L/mg) and qmax is the maximum adsorption quantity (mg/g).

Another dimensionless parameter, called the separation factor (R_L), whose expression is given by equation:

$$R_L = \frac{1}{1 + K_L * C_0} \quad \textbf{(8)}$$

Where C_0 is the initial concentration of the adsorbate (mg/L), and KL (L/mg) is the Langmuir constant.

This parameter is used to predict whether such a model is favorable or not, depending on its value defined by Hall and al. [29]: If $0 < R_L < 1$: the isotherm is favorable; if $R_L=1$: the isotherm is linear; if $R_L>1$: the isotherm is not favorable and if RL=0: the isotherm is irreversible.

Freundlich model: The Freundlich model is given by the empirical formula [11]:

$$q_e = k_F * C_e^{1/n} \qquad \textbf{(9)}$$

Where q_e is the concentration of the adsorbate (mg/g), Ce is often expressed in mg/L, K_F is a constant relative to the adsorption capacity (mg/g), n is the constant relative to the affinity between the adsorbate and the surface.

3. Result and discussion

3.1. Characterization of adsorbent

3.1. FTIR

The Fourier transform infrared spectroscopic analysis allows highlighting the chemical groups present in a given material, on figure 1 presents the infrared spectrum.

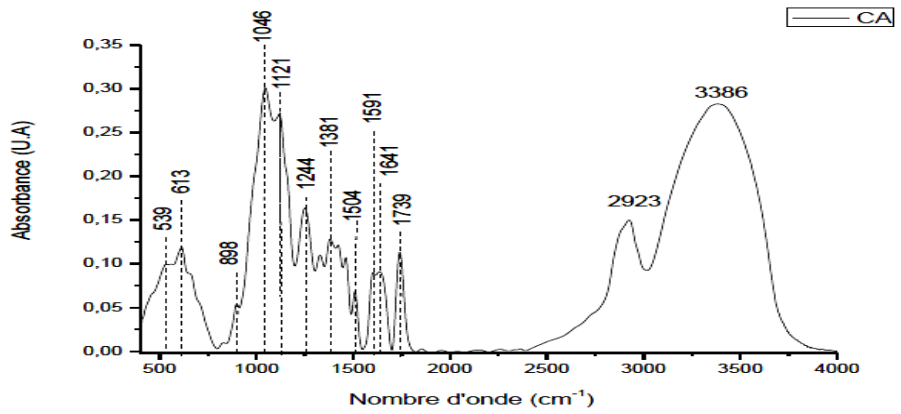

Figure 1: FTIR spectrum of almond shells

The infrared spectrum of almond shells showed two C-Cl elongations of alkyl and acid chlorides at 539 and 613 cm^{-1}, respectively. The 898 cm^{-1} band corresponding to the deformation of the N-H function of amines I and II. Intense C-O-elongation for the secondary alcohols CH-OH at 1121-1244 cm^{-1}, was due to C-O elongation (1046 cm-1), then followed by bond deformation of the phenols O-H at 1381 cm-1. Tertiobutyl group (-C $(CH_3)_3$) appeared (1381 cm^{-1}) [9]. In addition, at 1430-1455 cm^{-1}, a deformation bond of $-CH_2$ was revealed. An elongation of the aromatic C=C group alternated at 1504 cm^{-1}, the scissor movement of NH_2 caused a deformation at peaks 1591-1641cm^{-1} [10]. Subsequently, a very intense elongation of the carboxylic acids occurred at 1739 cm^{-1}, the aromatic derivatives are presented, between 2024 and 2371 cm^{-1}, by the "fingerprint" harmonic combination bands. An asymmetric elongation of the aliphatic C-H is apparent at 2923 cm^{-1}, it is followed by an O-H phenols elongation with a broad and intense band due to hydrogen bonding at 3386 cm^{-1} (of shell and water structure) [11]. All these resulting bands are in agreement with the composition of almond shells in terms of cellulose, hemicelluloses and lignin, major constituents of the shell (and of the plant biomass in general).

3.1.2 XRD

On the X-ray difragtogram we observe two main peaks appearing and located at 2 θ = 16.67° and 2 θ= 21.45° (figure.2), which characterizes the cellulose structure, these results are in agreement with the data of the literature [6]. Cellulose has a semi-crystalline structure; it has both disordered areas (amorphous areas) and highly ordered areas (crystalline areas) [12]. The non-crystallinity of some areas of cellulose is due to the existence of hydroxyl groups on the glucose which are amorphous [13]. Concerning the crystalline phase, other hydroxyl groups form numerous hydrogen bonds that arrange themselves in a vast network contributing directly to the compact crystal structure.

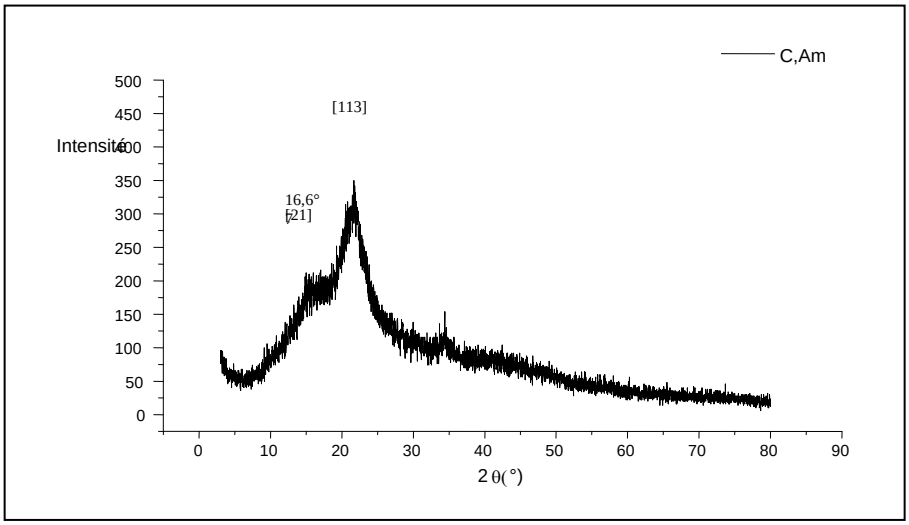

Figure 2: XRD of the almond shell

3.1.3 SEM

Scanning electron microscopy (SEM) was used to observe the morphology of the almond shell and illustrate the porosity. In order to highlight this porosity, the image was taken by SEM on the particles (0.3-0.7mm) of the almond shell. It is easy to see from the **figure 3** that the almond shell is a naturally porous material [6]. It is possibly possible that it has natural bioadsorption abilities without resorting to chemical or thermal activation. The Edx spectrum confirms the constituents of almond shell the existence of oxygen and carbon.

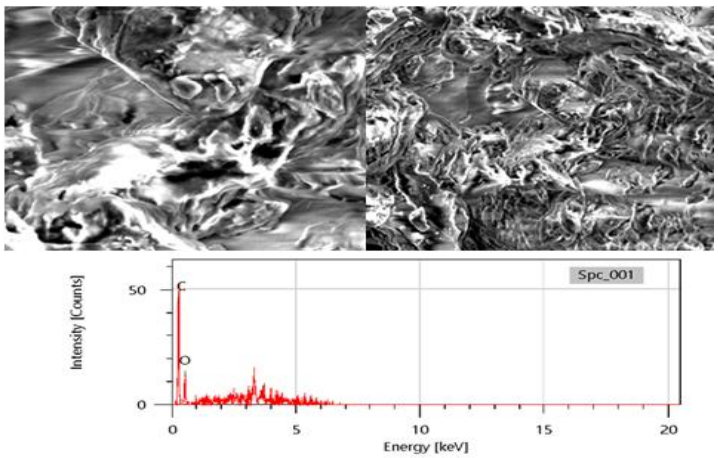

Figure 3: SEM images of almond shell and Edx

3.1.4 BET method

Textural parameters play an important role in the adsorption process; therefore, it is necessary to determine these parameters. The method of adsorption/desorption of N_2 allows to determine the specific surface of the almond shell which is equal to 1.3645 m²/g. Moreover, the adsorption isotherm is of type II (figure.4), according to the IUPAC classification [9].

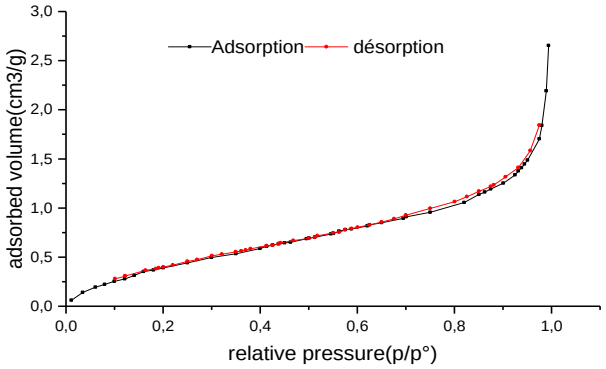

Figure 4: N_2 adsorption / desorption isotherm on the almond shell

3.1.5 Point of zero charge: pH_{pzc}

The PH_{PZC} is very important in adsorption phenomena, especially when electrostatic forces are involved in the mechanisms, which is the general case with bioadsorbents. The pH_{PZC} of material (the isoelectric point), is the point where the curve pH_{final} =f($pH_{initial}$) intercepts the line pH_{final} =$pH_{initial}$). According to figure 5, the point of intersection corresponds to pH_{pzc}=6.2. This parameter gives information on the dominant charge on the solid surface when the pH of the medium is varied [14].

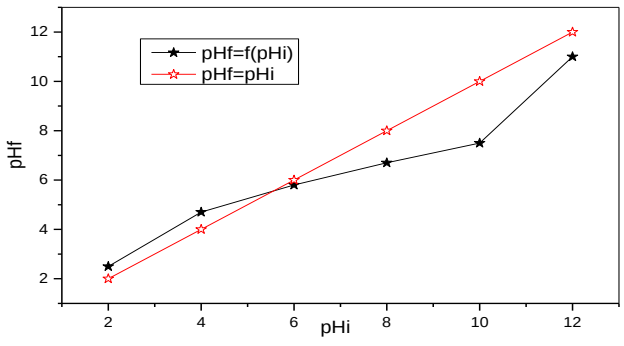

Figure 5: pH_{zero} charge point

3.2 Adsorption of methylene bleu

3.2.1 Effect of pH

The initial pH value of the colored solution is a very important parameter to control the adsorption process, and it has an impact on the adsorption capacity. It can change the surface charge of the adsorbent, the degree of ionization of the adsorbate, and the degree of dissociation of functional groups at the active site of the adsorbent [8], [15]. The result is shown in the figure. It can be seen from the figure 6 that as the pH value of the solution increases, the solid adsorption

capacity of BM increases significantly. The evolution of adsorption capacity in the studied pH range can be explained by the fact that when the pH is higher than the pH_{pzc} of the almond shell (pH_{pzc} = 6.2), the solid surface is negatively charged and the coloring molecules are cations (BM) in the solution positive charge [12], [16]. The adsorption can be considered by electrostatic interaction between the different charges of the solid and the dye. As the pH value increases, these interactions increase, because as the solution becomes more and more alkaline, the solid surface becomes more and more negative.

3.2.2 Effect of mass

The figure 7 gives us the amount of BM adsorbed at equilibrium as a function of the adsorbent mass. The graph shows that, in all cases, the percentage of decoloration increases with the mass of the adsorbent. This is easy to understand, as increasing the mass of the adsorbent will increase the specific surface area, thus increasing the number of available adsorption sites [15], resulting in an increase in the amount of dye adsorbed. Although the percentage of adsorption increases with increasing adsorbent dose, the decrease in the amount adsorbed per unit mass (mg/g) can be explained by the unsaturation of the adsorption site [9]. The curve in the figure shows that for the solid, the percentage of dye removal (BM) is in fact the total (100%).

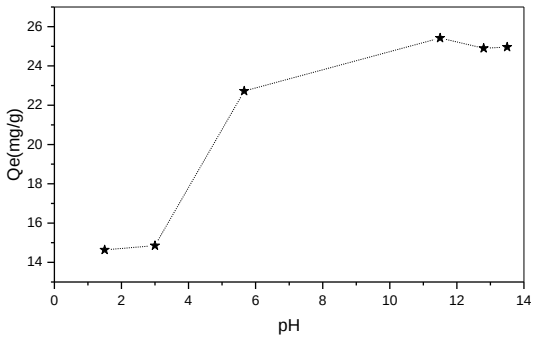

Figure 6: Effect of pH

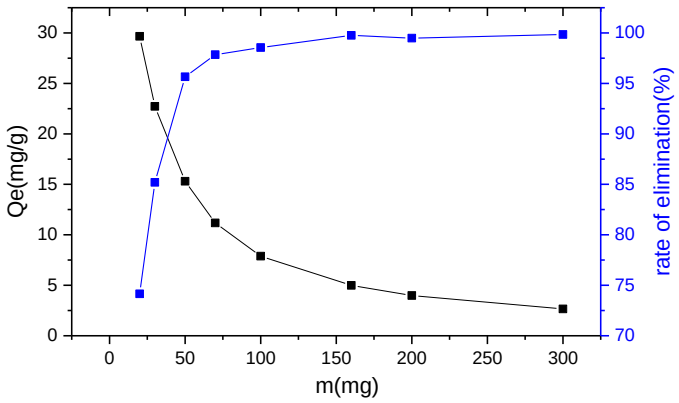

Figure 7: Effect of mass

3.2.3 Effect of temperature

It is well known that due to the decrease in solution viscosity, increasing the temperature will increase the rate of diffusion of adsorbate molecules through the outer boundary layer into the adsorbent particles [17]. This figure 8 shows the effect of temperature on the amount of methylene blue adsorption. It can be seen from the figure that

temperature has an effect on BM adsorption, indicating that the adsorption process is endothermic [2]. Although the increase in temperature promoted a small increase in the amount of methylene blue adsorption, it indicated that the increase in temperature had little effect on the adsorption of BM to solids. However, the process is endothermic and increasing the temperature will increase the mobility of BM molecules. Similar results are found for the adsorption of BM at different temperatures on palm grains [19] and the adsorption of BM on activated carbon [18].

3.2.4 Effect of initial concentration

The study of adsorption kinetics as a function of initial concentration shown in Figure 9 shows that for higher concentrations (24 mg/g), the adsorption capacity of methylene blue is better. We observed that the increase in the adsorption capacity of solid, which other studies have also observed. We noticed that for low concentration solutions, the equilibrium is reached after 20 minutes even for higher initial concentrations (40mg/L), the equilibrium is reached after 20 minutes. The percentages of discolorations for both concentrations are above 90%. Adsorption is rapid in the first few minutes of the reaction, which can be explained by the fact that at the beginning of adsorption, the number of active sites available on the surface of the adsorbent is much higher than the number of active sites remaining. For high contact times the molecule it needs time to diffuse inside the pore of the adsorbent, for the rest of the unabsorbed amount is interpreted by the saturation of the surface of the adsorbent (all adsorption sites are occupied) [20].

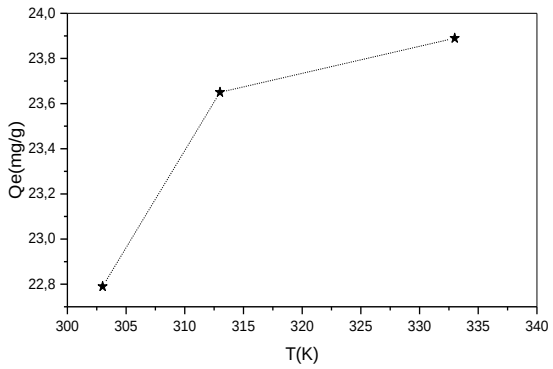

Figure 8: Effect of temperature

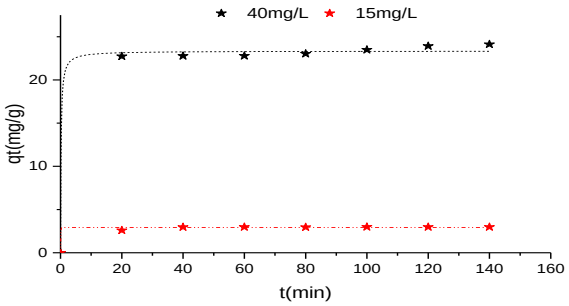

Figure 9: Effect of initial concentration

3.2.5 Effect of particle size

The figure shows that the adsorbed amount is high in the case of small grains (50<d<150), this amount undergoes a decrease in the large grain size d>200. This can be justified by the effect of intraparticle space on the penetration of dye molecules into the pores of the particles or probably due to the resistance to the transfer of material inside the

solid particles. Furthermore, it is well known that the smaller the particle diameter, the larger the specific surface area and therefore the larger the adsorbed amount, if we agree with the results of the figure 10.

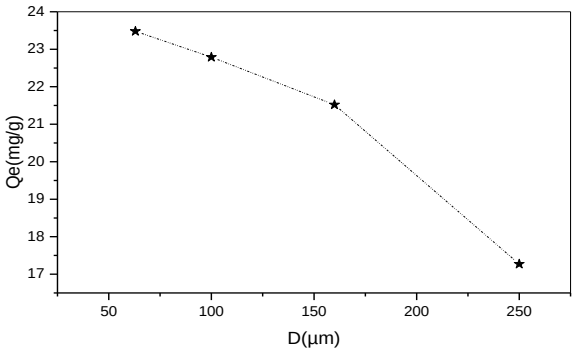

Figure 10: Effect of granulometry

3.2.6 Effect of the agitation speed

One of the first parameters studied concerns the influence of the agitation speed which plays a very important role in the control of agglomeration. From figure 11, we observe that the rate of adsorption depends on the speed of agitation, we notice that the more the speed of agitation increases the more the quantity adsorbed increases. This phenomenon may be due to the increase in the speed of agitation that affects the resistance to the transfer of material outside the particle [27], [28]. Moderate velocities give a good homogeneity of the suspension. At high speeds there is an appearance of the phenomenon of vortex which can cause heterogeneity of the suspension or decrease the adsorption capacity of dye molecules for this we are interested in a range of speed not exceeding 600 rpm.

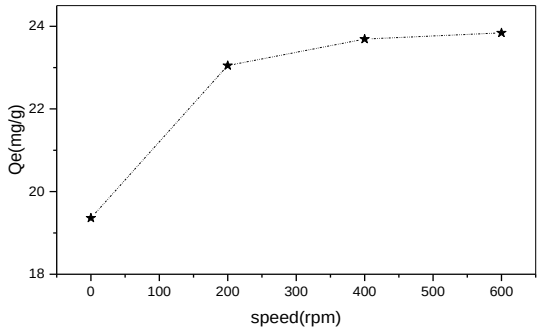

Figure 11: Effect of the agitation speed

3.2.7 Kinetic

Several kinetic models were used to interpret the experimental data, to give essential information for the use of this almond shell in the adsorption field. We have adopted three kinetic models: These models are: pseudo-first-order (PPO), pseudo-second-order (PSO) and intraparticle diffusion. The best model established for the study of adsorption kinetics is chosen according to the correlation factor. The higher this factor the more favorable the model is for the study of the adsorption process [4]. From the results of **Tables 1,** we notice that the model with the highest correlation factor is the pseudo-second-order model with a factor of R^2=0.998, so we can deduce that the pseudo-second-order model is the one that better describes the adsorption process of dye on the almond shell. Analysis of kinetic data by other researchers has also shown that the pseudo-second-order rate equation can simulate the adsorption of BM with

good agreement. We also note that the adsorbed amount calculated by this model is closer to experimental adsorbed amount [20]. From the figure 12, we notice that there are two different stages. The first part of the curve, which is the first stage, represents the diffusion of molecules into the solid. Generally, this is the longest stage. The second step represents the adsorption equilibrium where the reaction takes place. If intraparticle diffusion was the determining step in the adsorption process, then the corresponding line should pass through the origin. This is not the case that we observe in the Figure, so we can say that intraparticle diffusion is not the determining mechanism of the adsorption of the BM on the solid, it exists, but it takes place together with the adsorption of the BM. exists, but it takes place together with the other diffusion mechanisms. The intersection of the line corresponding to the intraparticle diffusion is proportional to the thickness of the boundary layer, same results found in the adsorption of BM by activated carbon prepared from coconut shell activated with NaOH [21], [22]. According to the Figure.12, we notice that there are two different stages. The first part of the curve, which is the first stage, represents the diffusion of the molecules in the solid. Generally, it is the longest stage. The second step represents the adsorption equilibrium where the reaction takes place. If the intraparticle diffusion was the determining step in the adsorption process then the corresponding line should pass through the origin.

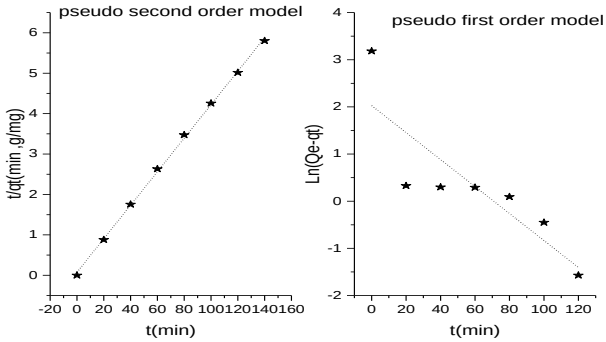

Figure 12: modeling of adsorption kinetics

What we observed in Figure 13 is not the case, then we can say that intraparticle diffusion is not the determining mechanism for BM adsorption on solids, it exists but occurs simultaneously because of adsorption of BM. exists, but it occurs concurrently with other diffusion mechanisms. The intersection of streets, reminiscent of intra-particle diffusion, is proportional to the thickness of the physical phenomenon, the same results were found in the adsorption of BM with walnut shells [21], [22].

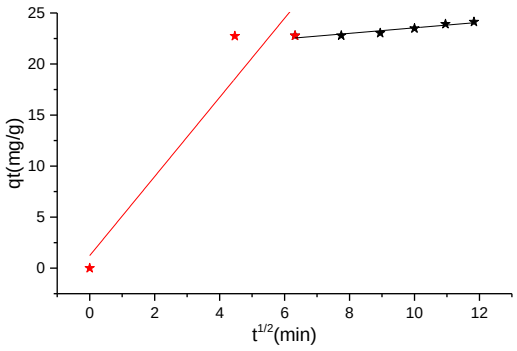

Figure 13: Intraparticle adsorption model

Table 1: Kinetic data of MB adsorption

	Parameter	
	T°C	30
	qtexp(mg/g)	24.02
Pseudo first order	**k1 (min-1)**	0.027
	qe (mg/g)	7.59
	R1	0.68
Pseudo second order	**k2 (g/mg.min)**	0.024
	qe (mg/g)	24.39
	R2	0.99

3.2.6 Modeling of adsorption isotherms

The parameters obtained from isotherm modeling provide important information about the adsorption mechanism, surface properties and adsorbent-adsorbate affinities. The two most commonly used two-parameter models are the Langmuir and Freundlich models. The best applicable model among those we have chosen will be evaluated from this R2 coefficient ($0 < R^2 < 1$) and the value of the maximum quantity obtained from the different models and that obtained experimentally [23], [25]. From the modeling results of the isotherms given in the table, we observe that the nonlinear models represent well the adsorption isotherms of BM on the solid Overall, we find that the Freundlich model is the most credible model that better describes our experimental results, with a correlation coefcient $R^2 = 0.99$. The Freundlich model assumes the formation of multilayers.

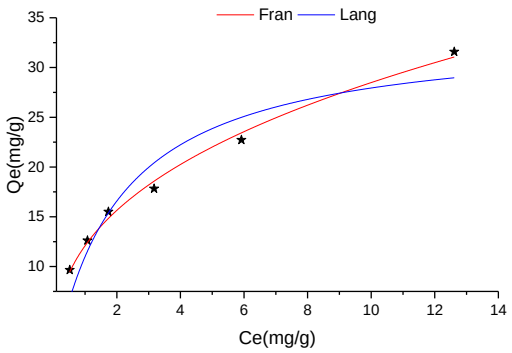

Figure 14: adsorption isotherm modeling

The parameter 1/n informs about the intensity of adsorption, or the strength of adsorption interactions. It also indicates the relative distribution of the energy sites for adsorption and depends on both the nature and the strength of the nature and strength of the adsorption process. The value of 1/n obtained is less than 1 which indicates an adsorption of physical nature. The value of RL (Table 2) obtained between 0 and 1 indicates that the adsorption process is favorable. The calculated true ultimate adsorption capacity (Q_m) obtained (Table 2) indicates that CM is a potential bioadsorbent for the removal of Methylene Blue from wastewater and can therefore be used for wastewater treatment and can therefore be used for wastewater treatment, and can therefore be used for wastewater treatment [4], [20], [26].

Table 2: Parameters of the adsorption isotherm models

Model	T (°C)	30
Langmuir	**q_m(mg/g)**	33.71
	K_L (L/mg)	0.48
	R^2	0.88
	χ^2	0.15
	R_L	0.083
Freundlich	**K_F (mg/g)**	12.09
	1/n	0.37
	R^2	0.99
	χ^2	0.35

3.2.9 Thermodynamic study

Thermodynamic parameters such as standard free enthalpy (ΔG°), standard enthalpy (ΔH°) and standard entropy (ΔS°) were determined using the following equations [27-30]: Table 3 gives the values of standard free enthalpy, standard enthalpy, and standard entropy, extrapolated from the straight form: full size form. The negative value of ΔG° indicates that the reaction is spontaneous, the value of ΔH° confirms the effect of the temperature on the adsorbed quantity (endothermic) and the value of ΔS° shows that the order of distribution of the molecules of the dye on the adsorbent decreases with respect to that in the solution [28,29]. The approach of the molecules from the solid phase, through the channels of the fibers, thus creates a more organized distribution. Moreover, the low value of the standard enthalpy (10kJ.mol^{-1}) clearly indicates that it is indeed a physisorption [31-33].

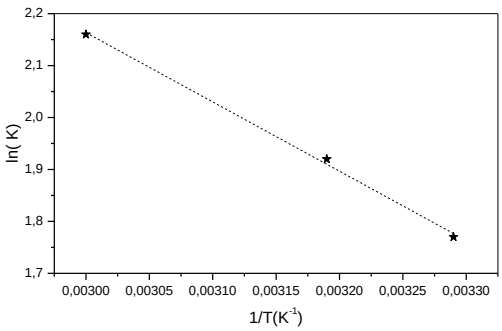

Figure 15: variation of Ln (K) as a function of 1/T

Table 3: Thermodynamic parameters

T(K)	ΔG° (kJ.mol^{-1})	ΔS° (J.mol^{-1} .K^{-1})	ΔH° (kJ.mol^{-1})
303	-4.460		
313	-5.362	49,10	10.284
333	-5.982		

3. Conclusion

In brief, the results show that the adsorbent almond shell has a porous structure with multiple chemical functional groups (O-H, C-H, C=N, C-C), which can adsorb chemical dyes. The adsorption parameters (dose effect, contact time, pH and temperature) have the optimal adsorption conditions and adsorption kinetic model for "almond shell"

aggregates were studied. After 20 minutes of contact, the "almond shell" aggregates have a 90% decoloration capacity in methylene blue solution (pH, dose ...). This result is very encouraging for testing other dyes and liquid rejects from the textile industry. Following the example of the objective of valorization of the by-product "almond shell" in the field of the treatment of waste water, tests of preparation of activated carbon almond shell with a better specific adsorption surface are in progress.

References

[1] Y. Dehmani, O. El Khalki, H. Mezougane, S. Abouarnadasse, "Comparative study on adsorption of cationic dyes and phenol by natural clays," *Chem. Data Collect.*, 33 (2021) 100674. http://doi.org/10.1016/j.cdc.2021.100674

[2] A. H. Jawad, A. S. Abdulhameed, "Mesoporous Iraqi red kaolin clay as an efficient adsorbent for methylene blue dye: Adsorption kinetic, isotherm and mechanism study," *Surfaces and Interfaces*, 18 (2019) 100422.

[3] R. R. Pawar, Lalhmunsiama, P. Gupta, S. Y. Sawant, B. Shahmoradi, S. M. Lee, "Porous synthetic hectorite clay-alginate composite beads for effective adsorption of methylene blue dye from aqueous solution" *Int. J. Biol. Macromol.*, 114 (2018) 1315–1324..

[4] H. Xue, "Adsorption of methylene blue from aqueous solution on activated carbons and composite prepared from an agricultural waste biomass: A comparative study by experimental and advanced modeling analysis," *Chem. Eng. J.*, 430(August 2021) (2022) 132801.

[5] M. Elharti, K. Legrouri, E. Khouya, H. Hannache, S. Fakhi, M. El boucchti, N. Hanafi, A. Solhy, B. Hammouti, Preparation of Adsorbent Material from Moroccan Oil Shele of Timahdit: Optimization of Parameters Processes and Adsorption Tests, *Der Pharma Chemica*, 4(5) (2012) 2130-2139

[6] C. Ad, M. Benalia, Y. Laidani, H. Elmsellem, F. Ben Saffedine, I. Nouacer, M. Djedid, B. El Mahi, B. Hammouti,Adsorptive removal of cadmium from aqueous solution by Luffa Cylindrica: Equilibrium, dynamic and thermodynamic, *Der Pharma Chemica*, 7N°12 (2015)388-397

[7] S. Çoruh, F. Geyikçi, E. Kiliç,U. Çoruh, "The use of NARX neural network for modeling of adsorption of zinc ions using activated almond shell as a potential biosorbent," *Bioresour. Technol.*, 151(2014)406–410.

[8] B. Ba Mohammed, "Insights into methyl orange adsorption behavior on a cadmium zeolitic-imidazolate framework Cd-ZIF-8: A joint experimental and theoretical study," *Arab. J. Chem.*, 14(1)(2021)102897.

[9] H. Ait Ahsaine , "Cationic dyes adsorption onto high surface area 'almond shell' activated carbon: Kinetics, equilibrium isotherms and surface statistical modeling," *Mater. Today Chem.*, 8 (2018) 121–132.

[10] F. Doulati Ardejani, K. Badii, N. Y. Limaee, S. Z. Shafaei, A. R. Mirhabibi, "Adsorption of Direct Red 80 dye from aqueous solution onto almond shells: Effect of pH, initial concentration and shell type," *J. Hazard. Mater.*, 151,(2–3) (2008) 730–737.

[11] N. Maaloul, P. Oulego, M. Rendueles, A. Ghorbal, M. Díaz, "Novel biosorbents from almond shells: Characterization and adsorption properties modeling for Cu(II) ions from aqueous solutions," *J. Environ. Chem. Eng.*, 5(3) (2017) 2944–2954.

[12] I. Loulidi, F. Boukhlifi, M. Ouchabi, A. Amar, M. Jabri, A. Kali, and C. Hadey, "Assessment of Untreated Coffee Wastes for the Removal of Chromium (VI) from Aqueous Medium," *Int. J. Chem. Eng.*, (2021) (2021) 9977817. https://doi.org/10.1155/2021/9977817

[13] I. Loulidi., "Adsorption of Crystal Violet onto an Agricultural Waste Residue: Kinetics, Isotherm, Thermodynamics, and Mechanism of Adsorption," *Sci. World J.*, 2020(April 2020) (2020) 5873521.

[14] A. Dehbi , "Comparative study of malachite green and phenol adsorption on synthetic hematite iron oxide nanoparticles (α-Fe2O3)," *Surfaces and Interfaces*, 21(June) (2020)100637.

[15] A. Amar, I. Loulidi, A. Kali, F. Boukhlifi, C. Hadey, and M. Jabri, "Physicochemical Characterization of Regional Clay: Application to Phenol Adsorption," *Appl. Environ. Soil Sci.*, vol. 2021 (2021).

[16] H. Asnaoui, Y. Dehmani, M. Khalis, E. K. Hachem, "Adsorption of phenol from aqueous solutions by Na–bentonite: kinetic, equilibrium and thermodynamic studies," *Int. J. Environ. Anal. Chem.*, 6 (2020) 1–15.

[17] A. Gładysz-Płaska, M. Majdan, S. Pikus, D. Sternik, "Simultaneous adsorption of chromium(VI) and phenol on natural red clay modified by HDTMA," *Chem. Eng. J.*, 179(2012),140–150.

[18] F. Bensafiddine, M. Benalia, A. Seyd, M. Djedid," Biosorption of heavy metals (Cooper , Nickel) and dye (methylene bleu) from aqueous solution onto southern Algerian carob shells." *Moroccan Journal of Chemistry*, 3 (2020) 638–646.

[19] M. A. Behnajady , S. Bimeghdar, "Synthesis of mesoporous NiO nanoparticles and their application in the

adsorption of Cr(VI)," *Chem. Eng. J.*, 239 (2014) 105–113.
[20]S. S. Vedula, G. D. Yadav, "Wastewater treatment containing methylene blue dye as pollutant using adsorption by chitosan lignin membrane: Development of membrane, characterization and kinetics of adsorption," *J. Indian Chem. Soc.*, 5 (2021) 100263.
[21] H. Wang, "Effective adsorption of dyes on an activated carbon prepared from carboxymethyl cellulose: Experiments, characterization and advanced modelling," *Chem. Eng. J.*, 417 (2021) 128116.
[22] S. F. Lütke, A. V. Igansi, L. Pegoraro, G. L. Dotto, L. A. A. Pinto, and T. R. S. Cadaval, "Preparation of activated carbon from black wattle bark waste and its application for phenol adsorption," *J. Environ. Chem. Eng.*, 7(5) (2019) 103396.
[23] Y. Yasin, M. Hussein, and F. Ahmad , "Adsorption of methylene blue onto treated activated carbon," *Malaysian J. Anal. Sci.*, 11(2) (2007) 400–406.
[24] R. Hana., "Adsorption of methylene blue by phoenix tree leaf powder in a fixed-bed column: experiments and prediction of breakthrough curves," *Desalination*, 245 (2009) 284–297
[25] N. Hassan, A. Shahat, A. El-Didamony, A. El-Desouky," Equilibrium, Kinetic and Thermodynamic studies of adsorption of cationic dyes from aqueous solution using ZIF-8.", *Moroccan Journal of Chemistry*, 8(3) (2020) 624–635.
[26] S. Jodeh, J. Amarah, S. Radi, O. Hamed, I. Warad, "Removal of Methylene Blue from Industrial Wastewater in Palestine Using Polysiloxane Surface Modified with Bipyrazolic Tripodal Receptor. *Moroccan Journal of Chemistry*, 1 (2016) 140–156.
[27] M. Ouhammou, L. Lahnine, S. Mghazli, " Green chemistry for treatment of liquid discharges from a dyeing industry : bio coagulation and flocculation". *Moroccan Journal of Chemistry*, 3 (2021) 684–694.
[28] H. Yemendzhiev, H. Koleva, R. Zerrouq, F. Nenov, Utilization of Olive Mill Waste in Microbial Electrolysis Cell. *Moroccan Journal of Chemistry*, 9(1) (2021) 01–06.
[29] J. Krstić, Z. Mojović, A. A. Rabi, D. Lončarević, N. Vukelić, D. Jovanović, "Adsorption of methylene blue from aqueous solution onto bentonite," *Environ. Earth Sci.*, (2011) 1097–1106.
[30] Y. Kuang, X. Zhang, S. Zhou, "Adsorption of methylene blue in water onto activated carbon by surfactant modification," *Water (Switzerland)*, 12(2) (2020) 1–19.
[31] M. A. Adebayo, F. I. Areo, "Removal of phenol and 4-nitrophenol from wastewater using a composite prepared from clay and Cocos nucifera shell: Kinetic, equilibrium and thermodynamic studies," *Resour. Environ. Sustain.*, 3 (2020) 100020
[32] G. S. dos Reis, "Removal of Phenolic Compounds from Aqueous Solutions Using Sludge-Based Activated Carbons Prepared by Conventional Heating and Microwave-Assisted Pyrolysis," *Water. Air. Soil Pollut.*, 228(1) (2017) 1–17.
[33] Y. Dehmani, S. Abouarnadasse, "Study of the adsorbent properties of nickel oxide for phenol depollution," *Arab. J. Chem.*, 13(1) (2020) 5312–5325.